JPET Fast Forward. Published on November 12, 2018 as DOI: 10.1124/jpet.118.249789
This article has not been copyedited and formatted. The final version may differ from this version.

Experimental evidence for re-secretion of PGE_2 across rat alveolar epithelium by OATP2A1/S*LCO2A1*-mediated transcellular transport

Takeo Nakanishi*, Hiroki Takashima, Yuka Uetoko, Hisakazu Komori and Ikumi Tamai

Affiliation

Faculty of Pharmaceutical Sciences, Institute of Medical, Pharmaceutical and Health Sciences, Kanazawa University, Kanazawa 920-1192, Japan.

JPET Fast Forward. Published on November 12, 2018 as DOI: 10.1124/jpet.118.249789
This article has not been copyedited and formatted. The final version may differ from this version.

Running Title

Cellular disposition of PGE_2 in alveolar epithelial cells

Corresponding author

Takeo Nakanishi, Ph.D.

Faculty of Pharmaceutical Sciences, Institute of Medical, Pharmaceutical and Health Sciences,

Kanazawa University, Kakuma-machi, Kanazawa 920-1192, Japan,

Tel: +81-76-234-4421, Fax: +81-76-264-6284

E-mail: nakanish@p.kanazawa-u.ac.jp

Number of pages: 29

Number of tables: 2

Number of figures: 7

Number of references: 37

Number of words in the Abstract: 250

Number of words in the Introduction: 479

Number of words in the Discussion: 1371

List of Nonstandard Abbreviations: AEL; alveolar epithelial lining, AP; apical, AT1; type 1 alveolar epithelial, AT2; type 2 alveolar epithelial, BL; basolateral, BSP; bromosulfophthalein.

Recommended Section: Metabolism, Transport, and Pharmacogenomics

Conflict of Interest: None of the authors declare any conflict of interest.

JPET Fast Forward. Published on November 12, 2018 as DOI: 10.1124/jpet.118.249789
This article has not been copyedited and formatted. The final version may differ from this version.

Abstract

Prostaglandin transporter Oatp2a1/*Slco2a1* is expressed at the apical (AP) membranes of type-1 alveolar epithelial (AT1) cells. To investigate the role of OATP2A1 in PGE_2 handling by alveolar epithelium, we studied PGE_2 transport across and secretion from monolayers of rat AT1-like (AT1-L) cells obtained by trans-differentiation of type-2 alveolar epithelial cells (AT2) isolated from male Wistar rats. Rat AT1-L cells expressed Oatp2a1/*Slco2a1*, together with smaller amounts of Mrp4/*Abcc4* and Oct1/*Slc22a1*. PGE_2 uptake was saturable with Km 43.9 ± 21.9 nM. Transcellular transport of PGE_2 across AT1-L cells grown on permeable filters in the AP-to-basolateral (BL) direction was 5-fold greater than that in the reverse direction, and was saturable with Km 118 ± 26.8 nM; it was significantly inhibited by OATP inhibitors, bromosulfophthalein (BSP) and suramin, and an MRP4 inhibitor, ceefourin-1. The effects of BSP on the distribution of PGE_2 produced by bradykinin-treated AT1-L cells and PGE_2-d_4 externally added on the AP side of the cells were simultaneously monitored. In the presence of BSP, PGE_2 increased more rapidly on the AP side, while PGE_2-d_4 decreased more slowly on the AP side. The decrease in PGE_2-d_4 from the AP side corresponded well to the increase on the BL side, indicating that intracellular metabolism did not occur. These results suggest that Oatp2a1 and Mrp4 mediate transepithelial transport of PGE_2 in the AP-to-BL direction. Therefore, OATP2A1 may be an important regulator of PGE_2 in alveolar epithelium by reducing secretion of PGE_2 and facilitating "re-secreting" PGE_2 present in the alveolar lumen to the interstitial space or blood.

Introduction

There is significant evidence that PGE_2 exhibits anti-fibrotic action in the lungs. *In vitro* studies suggest that PGE_2 suppresses various metabolic capabilities of fibroblasts, including collagen production and trans-differentiation to myofibroblasts (**Kolodsick et al., 2003; Moore et al., 2005; Huang et al., 2007**), resulting in increased sensitivity of fibroblasts to apoptosis. Thus, insufficient PGE_2 generation has been suggested to contribute to pulmonary fibrosis (**Maher et al., 2010**). This notion is supported by evidence that *Cox-2* deficient mice are more susceptible to bleomycin-induced fibrosis (**Keerthisingam et al., 2001; Bonner et al., 2002**); however, eicosanoids other than PGE_2 (e.g. PGI_2 and $PGF_{2\alpha}$) are also claimed to play a role in the progression of pulmonary fibrosis (**Lovgren et al., 2006; Oga et al., 2009**). PGE_2 is present as an organic anion under physiological conditions and requires an uptake carrier to be reimported (**Sekine et al., 1997; Schuster, 1998; Tamai et al., 2000; Kimura et al., 2002; Gose et al., 2016**). Indeed, OATP2A1 encoded by *SLCO2A1* has been characterized as a high-affinity prostaglandin uptake transporter (**Kanai et al., 1995; Chan et al., 1998**) and measurements of its intra- and extra-cellular concentration indicate that it plays a role in PGE_2 signaling (**Chi et al., 2006; Chi et al., 2008; Syeda et al., 2012; Nakanishi et al., 2017**).

OATP2A1 is abundantly expressed in the lungs of rodents and humans (**Kanai et al., 1995; Lu et al., 1996; Pucci et al., 1999; Chang et al., 2010**), especially in endothelial cells, where it mediates rapid clearance of PGE_2 from the systemic circulation through the pulmonary vascular beds (**Ferreira and Vane, 1967**). We recently found that OATP2A1 is expressed in type 1 alveolar epithelial (AT1) cells in mouse lung, as well as primary-cultured rodent AT1 cell-like (AT1-L) cells, and that pulmonary fibrosis was more severe in intra-tracheally BLM-administered *Slco2a1*-null mice (*Slco2a1*$^{-/-}$), which show lower and higher concentrations of PGE_2 in lung tissue and alveolar lumen, respectively, compared to *Slco2a1* wild-type mice (*Slco2a1*$^{+/+}$) (**Nakanishi et al., 2015**).

JPET Fast Forward. Published on November 12, 2018 as DOI: 10.1124/jpet.118.249789
This article has not been copyedited and formatted. The final version may differ from this version.

Thus, our previous results suggest that OATP2A1 regulates the pulmonary distribution of PGE_2 produced by epithelial cells and inflammatory cells in the lumen of alveoli. Nevertheless, it is not fully understood how OATP2A1 is involved in PGE_2 handling by alveolar epithelial cells.

In the present study, alveolar type 2 epithelial (AT2) cells prepared from Wistar rats were trans-differentiated into AT1 cell-like (AT1-L) cells, and the function of OATP2A1 in AT1-L cells was characterized by means of cellular uptake and transcellular transport studies of native PGE_2 and externally applied [^{3}H]PGE_2 and PGE_2-d_4. The effects of an OATP2A1 inhibitor, bromosulfophthalein (BSP), were also examined. Our results suggest a role of OATP2A1 in transcellular transport of PGE_2 across AT1 cells in the direction from the alveolar lumen (AP side) to the interstitial space (BL side). Thus, OATP2A1 may mediate the redisposition of secreted PGE_2 in the lumen of alveoli to the interstitial space for re-use.

Material and Methods

Materials

[5,6,8,11,12,14,15-^{3}H]PGE_2 ([^{3}H]PGE_2; 163.6 Ci/mmol), and unlabeled and deuterium-labeled PGE_2 (PGE_2-d_4) were purchased from PerkinElmer Life Science (Boston, MA) and Cayman Chemical (Ann Arbor, MI), respectively. Bromosulfophthalein (BSP), suramin, and ceefourin-1 were obtained from Sigma-Aldrich (St. Louis, MO), Tokyo Chemical Industry (Tokyo, Japan), and Abcam (Cambridge, UK), respectively. All other compounds were commercial products of reagent grade from Sigma-Aldrich, FUJIFILM Wako Pure Chemical Corporation (Osaka, Japan), Thermo Fisher Scientific (Waltham, MA), Kanto Chemical (Tokyo, Japan), and Nacalai Tesque (Kyoto, Japan).

Preparation of ATI-L cells from isolated AT2 cells from rats

Animal studies were approved by the Committee for the Care and Use of Laboratory Animals of Kanazawa University and conducted in accordance with its guidelines (AP-143148 and -183945). Male Wistar rats (170–210 g body weight, at the age of 7 weeks) were i.p. injected with pentobarbital sodium (50 mg/kg), and given heparin (150 U, Mochida Pharmaceutical Co., Ltd., Tokyo, Japan) via the jugular vein. AT2 cells were prepared as previously described (**Richards et al., 1987; Ikehata et al., 2008**). A cannula was made in the trachea after tracheotomy, and the postcaval vein was cut. Subsequently, the lungs were perfused with Solution I (136.9 mM NaCl, 8.1 mM Na_2HPO_4, 1.5 mM KH_2PO_4, 2.7 mM KCl, 0.2 mM EDTA-2Na, 0.2 mM EGTA, pH 7.2) through the right ventricle and excised, and the bronchia and alveoli were rinsed several times to remove contaminating inflammatory cells. The lungs were filled with solution III (RPMI1640 medium obtained from FUJIFILM Wako Pure Chemical Corporation, containing 25 mM HEPES and 24 mM $NaHCO_3$), and then placed in physiological saline. Solution III containing trypsin (0.25%) was allowed to flow continuously from the cannula into the lungs for 30 min at 37°C. The trachea, bronchi and large airways were removed, and the lung tissues were minced into small pieces and then treated with Solution III containing DNase I (250 μg/mL) and tylosin (120 μg/mL). The resultant tissue and cell suspension were filtered through sterile gauze, and nylon net filters of 70 μm (Corning, Corning, NY) and 15 μm (Tanaka Sanjiro, Fukuoka, Japan) pore size. The filtered cell suspension was overlaid on high-density (1.089 g/mL) and low-density (1.040 g/mL) Percoll solutions as previously described (**Ikehata et al., 2008**), and AT2 cells were obtained by centrifugation at 250 × g and 4°C for 20 min. The cells were re-suspended in Solution I, and stained with trypan blue to confirm viability. AT2 cells from preparations with a viability of over 90% were cultured for 6 days in Dulbecco's modified Eagle's medium (DMEM) supplemented with 10% fetal bovine serum (FUJIFILM Wako Pure Chemical Corporation) at 37°C under an atmosphere of 5% CO_2 in air.

JPET Fast Forward. Published on November 12, 2018 as DOI: 10.1124/jpet.118.249789
This article has not been copyedited and formatted. The final version may differ from this version.

PGE_2 uptake by rat AT1-L cells and HEK/2A1 cells expressing human OATP2A1

For apical uptake studies, AT2 cells were seeded on multiple tissue culture plates (2×10^5 cells/cm^2) for 6 days, and then used for [^{3}H]PGE_2 uptake in the absence or presence of an OATP inhibitor as described before (**Nakanishi et al., 2015**). HEK293 cells transfected with *SLCO2A1* gene (HEK/2A1) were prepared for uptake assay as described previously (**Gose et al., 2016**). Intracellular accumulation of [^{3}H]PGE_2 was evaluated by measuring radioactivity in cell lysates with a liquid scintillation counter (Hitachi Aloka Medical, Tokyo, Japan); results are shown as cell-to-medium ratio normalized by protein content (μL/mg protein). The Michaelis constant (K_m) and the maximal rate of uptake (V_{max}) were obtained by fitting the data to the following equation,

$$v = \frac{V_{max} \times S}{K_m + S} \qquad (1)$$

where v and S are the uptake rate and the initial concentration of PGE_2, respectively. Kinetic parameters K_m and V_{max} were estimated by means of nonlinear least-squares analysis using KaleidaGraph (ver 4.0J, Hulinks, Tokyo, Japan).

PGE_2 transcellular transport across and secretion from rat AT1-L cells

AT1-L cells were plated on fibronectin (1 μg/well, Sigma-Aldrich)-coated Transwell filter membrane inserts with a 0.4 μm pore size and 6.5 mm diameter (Becton Dickinson, Franklin Lakes, NJ) at a density of 2.0×10^5 cells/well for 6 days. The cells were preincubated for 15 min at 37°C with transport medium (4.8 mM KCl, 125 mM NaCl, 1.2 mM KH_2PO_4, 1.2 mM $CaCl_2$, 1.2 mM $MgSO_4$, 5.6 mM glucose, 25 mM HEPES, pH 7.4, adjusted with NaOH). Basically, cells grown on filters with transepithelial electrical resistance of 500 (Ω·cm^2) or more were used for transport study. Transport was initiated by adding transport medium containing [^{3}H]PGE_2 (2.78 nM; e.g. 0.5 μCi/mL) or deuterium-labeled PGE_2 (PGE_2-d_4) and/or [^{14}C]mannitol (0.5 μCi/mL) to the AP (250

JPET Fast Forward. Published on November 12, 2018 as DOI: 10.1124/jpet.118.249789
This article has not been copyedited and formatted. The final version may differ from this version.

μL) or BL (1000 μL) side in the presence or absence of an inhibitor of the transporter of interest on both sides. To analyze PGE_2 secretion, endogenous PGE_2 was measured in DMEM without fetal bovine serum on both sides of cells treated with bradykinin (10 μM), which is an inducer of prostaglandin synthesis. At the designated time, transport medium was withdrawn for measurement from the AP (10 μL) and BL (100 μL) sides, and supplemented with an equal volume of medium with the same composition, except for PGE_2. At the end of assay, the filter membrane was washed with ice-cold transport medium and the cells were collected to measure the intracellular content of substrate. Radioactivity in the samples was quantified with a liquid scintillation counter (Hitachi Aloka Medical). Unlabeled or deuterium-labeled PGE_2 was quantified with LC-MS/MS as described below. The apparent permeability of PGE_2 across the cell monolayer was calculated as permeability coefficient (P_c, cm/sec) using the following equation,

$$P_c = \frac{\left(\frac{dQ}{dt}\right)}{A \times S} \qquad (2)$$

where Q, S and A are the amount of PGE_2 over a period of time t, the surface area of the filter membrane, and the initial concentration on the donor side, respectively.

PGE_2 measurements in the culture media and cell lysate

PGE_2 and PGE_2-d_4 were extracted from culture media and cell lysate into ethyl acetate containing formic acid (v/v, 0.24%) under acidic conditions; $PGF_{2\alpha}$-d_4 was used as an internal standard. The combined organic phase was dried under reduced pressure, reconstituted with acetonitrile containing 0.1% formic acid for analysis, and subjected to LC-MS/MS using an LCMS8050 triple quadrupole mass spectrometer (Shimadzu Co., Kyoto, Japan) coupled with an LC-30AD ultra-fast liquid chromatography system (Shimadzu Co.). The flow rate of the mobile phase was 0.3 mL/min and the injection volume was set as 30 μL. Luna® (C18, 20 × 4.0 mm, 3 μm, Phenomenex, Torrance,

CA) was used as an analytical column. Samples were kept at 4°C during the analysis. Electrospray negative ionization was used, and the mass transitions were monitored at m/z 351.00/271.35 for PGE_2, m/z 355.1/319.25 for PGE_2-d_4 and m/z 357.10/313.25 for d4-$PGF_{2\alpha}$. Analyst software Lab Solution LCMS was used for data manipulation.

RT-PCR

Total RNA was extracted from AT1-L cells using RNAiso Plus® (Takara Bio, Tokyo, Japan) and then reverse-transcribed to cDNA with M-MLV reverse transcriptase (Promega, Madison, WI). mRNA expression of 11 rat transporter genes was evaluated with the respective sequence primers (listed in Supplementary Table I). PCR products were visualized on 1.5% agarose gel with ethidium bromide.

Western blotting

Western blot analysis was performed as described previously (Shimada et al., 2015). The cells were homogenized by sonication (QSonica, LLC., Newtown, CT) and lysed in RIPA buffer (150 mM sodium chloride, 1% Nonidet P (NP)-40, 0.5% sodium deoxycholate, 0.1% SDS, and 50 mM Tris at pH 8.0) containing protease inhibitor cocktail (Nacalai Tesque). For Oatp2a1 and Mrp4, cells were lysed with M-PER buffer (Life technologies, Carlsbad, CA). Lysates were separated from nuclei and unbroken cells by centrifugation (10,000 × g), at 4 °C for 10 min, and protein concentration was determined using a Bio-Rad protein assay kit. A 20 - 40 μg aliquot of the total cell lysate was separated in SDS polyacrylamide gel (8 or 10%) and then electrotransferred onto a polyvinylidene difluoride membrane (Merck Millipore, Burlington, MA). The membranes were treated with 5% nonfat dry milk in TBS-T (0.1% Tween 20-containing Tris-buffered saline) to block non-specific binding for 1 hr at room temperature, and then incubated overnight at 4 °C with antibody diluted in

5% nonfat dry milk in TBS-T using primary antibodies against Cox-2, 15-Pgdh (1:250 dilution, Cayman Chemical), and Gapdh (1:5,000 dilution, Cell Signaling Technology, Danvers, MA). Anti-Oatp2a1 (1:1,000 dilution, Atlas Antibodies, Stockholm, Sweden) and anti-Mrp4 (1:1,000 dilution, Vector Laboratories, Burlingame, CA) antibodies were used with Immobilon® signal enhancer (Merck Millipore). The membrane was treated with HRP-conjugated anti-rabbit secondary antibody (1:2000 - 1:5000 dilution, Life Technologies) for 1 hr at room temperature and bands were revealed with ImmunoStar Zeta® (FUJIFILM Wako Pure Chemical Corporation). For Mrp4, the membranes incubated with primary antibody were reacted with biotin-conjugated goat anti-rabbit IgG (1:2,000, Vector laboratories) for 2 hr at room temperature, and then treated with HRP-conjugated streptavidin (1:2,000, Thermo Fisher Scientific, Waltham, MA) for 1 hr at room temperature. The signal was developed as described above. Bands of interest on the blots were analyzed using a CS analyzer (ATTO, Tokyo, Japan).

Statistical analysis

The statistical significance of differences was analyzed by means of Student's t-test or one-way ANOVA with Bonferroni's multiple comparison test. Multiple comparison was performed with Excel Toukei ver 2.03 software (Social Survey Research Information Co., Ltd., Tokyo, Japan). A p-value < 0.05 was considered significant.

Results

Expression of functional OATP2A1 in rat AT1-L cells.

mRNA expression levels of 11 genes encoding transporters that recognize prostaglandins as substrates were examined in AT1-L cells by means of RT-PCR (**Fig. 1**). mRNA expression of Oatp2a1 was almost exclusively found in AT1-L cells, and Oct1 and Mrp4 were faintly expressed.

JPET Fast Forward. Published on November 12, 2018 as DOI: 10.1124/jpet.118.249789
This article has not been copyedited and formatted. The final version may differ from this version.

Oatp2a1 is highly and moderately expressed in rat lung and kidney, respectively (**Kanai et al., 1995**), but the expression of Mrp4 is vice versa (**Chen and Klaassen, 2004**). Protein expression of Oatp2a1 and Mrp4 in AT1-L cells was assessed by Western blot analysis with homogenates of rat lung and kidney. The blots showed specific bands corresponding to Oatp2a1 (65 kDa) and Mrp4 (120 kDa) in AT1-L cells as detected in lung and kidney, respectively (**Figs. 1B and C**). Initial apical uptake of PGE_2 (determined at 2 min) by AT1-L cells grown on plates was saturable, and K_m and V_{max} were estimated as 43.9 ± 21.9 nM and 0.77 pmol/2 min/mg protein, respectively (**Fig. 2A**). An Eadie-Hofstee plot (inset of **Fig. 2A**) revealed a single saturable component. Apical uptake of $[^3H]PGE_2$ was significantly decreased in the presence of unlabeled PGE_2, a pan-OATP inhibitor BSP, or a selective OATP2A1 inhibitor TGBz 34A (TGBz) at 25 μM (Chi et al., 2006) and no significant difference was detected among the uptakes in the presence of these three inhibitors (**Fig. 2B**, one-way ANOVA with Bonferroni's multiple comparisons test, p-value > 0.05). Thus, since the inhibitory potential of BSP on PGE_2 uptake was comparable to that of TGBz in AT1-L cells, BSP was utilized as an OATP2A1 inhibitor in the following experiments.

Transcellular transport of PGE_2 across AT1-L cells

The AP-to-BL and BL-to-AP permeability of $[^3H]PGE_2$ was measured in rat AT1-L cells cultured on permeable filters. **Fig. 3A** shows time course of transcellular transport of $[^3H]PGE_2$ in the AP-to-BL direction. Permeated radioactivity on the BL side increased linearly for 40 min, and was significantly reduced by 73.0% in the presence of BSP, which is similar to the effect on initial uptake of PGE_2 from the AP side. The cellular permeability values of PGE_2 AP-to-BL transport ($P_{c,A\rightarrow B}$) were calculated as 4.27 and 0.83 $\times 10^{-5}$ cm/sec in the absence (control) and in the presence of BSP, respectively (**Fig. 3B**), whereas $P_{c,A\rightarrow B}$ of mannitol, a marker for para-cellular transport, corresponded to only 4.0% of the control $P_{c,A\rightarrow B}$ of PGE_2, and was not affected by BSP. The P_c in

JPET Fast Forward. Published on November 12, 2018 as DOI: 10.1124/jpet.118.249789
This article has not been copyedited and formatted. The final version may differ from this version.

the reverse direction ($P_{c,B\rightarrow A}$) of PGE_2 (0.71×10^{-5} cm/sec) was almost 5 times lower than its $P_{c,A\rightarrow B}$, (4.27×10^{-5} cm/sec), but was still higher than $P_{c,B\rightarrow A}$ of mannitol (0.27×10^{-5} cm/sec). Because $P_{c,B\rightarrow A}$ of PGE_2 was not reduced by BSP, the contribution of OATP2A1 to BL-to-AP transport of PGE_2 appears to be negligible (**Fig. 3B**). The AP-to-BL transport of PGE_2 was saturable with a Km of 118 ± 26.8 nM (**Fig. 3C**). Moreover, $P_{c,A\rightarrow B}$ of PGE_2 was significantly reduced in the presence of TGBz or suramin, which was used as a more selective inhibitor of OATP2A1 (**Kamo et al., 2017**). $P_{c,A\rightarrow B}$ of PGE_2 measured in the presence of a pan-inhibitor of OCTs, tetraethylammonium (TEA), was significantly higher than that with TGBz or suramin, but was not different from that in the absence of inhibitor (**Fig. 3D**, one-way ANOVA with Bonferroni's multiple comparisons). Furthermore, PGE_2 is exported by MRP4 (**Reid et al., 2003**); therefore, we further examined the effect of ceefourin-1, a specific inhibitor of MRP4 (**Cheung et al., 2014**), on transcellular PGE_2 transport. The $P_{c,A\rightarrow B}$ of PGE_2 was somewhat reduced by ceefourin-1 (**Fig. 4A**), but increasing concentrations of ceefourin-1 did not cause any statistically significant changes of OATP2A1-mediated PGE_2 uptake in HEK/2A1 cells (**Fig. 4B,** one-way ANOVA with Bonferroni's multiple comparisons test, p-value > 0.05). These results suggest that MRP4 may make only a minor contribution to PGE_2 efflux at the BL membranes of AT1-L cells.

Impact of OATP2A1 inhibitor on PGE_2 disposition in rat AT1-L cells

We further explored the role of OATP2A1 in PGE_2 handling by alveolar epithelium, where secretion, reuptake, transcellular transport and metabolism of PGE_2 synthesized by not only alveolar epithelial cells, but also other type of cells, all occur simultaneously. First, expression of rate-limiting enzymes of PGE_2 synthesis and metabolism was examined in rat AT1-L cells. Western blot analysis showed constitutive expression of Cox-2 and 15-Pgdh in AT1-L cells at significant levels (**Fig. 5**). Indeed, 15-ketoPGE_2, which is a metabolite of PGE_2 produced by 15-PGDH, was found in

JPET Fast Forward. Published on November 12, 2018 as DOI: 10.1124/jpet.118.249789
This article has not been copyedited and formatted. The final version may differ from this version.

AT1-L cells grown on filters when they were treated with an inflammatory mediator, bradykinin, in order to induce PGE_2 synthesis. Furthermore, to mimic the disposition of PGE_2 produced by cells other than AT1 cells in alveolar epithelial lining (AEL) fluid, PGE_2-d_4 (20 nM) was externally added on the AP side of bradykinin-treated AT1-L cells, and the effects of BSP on the distributions of PGE_2-d_4 and endogenous PGE_2 were simultaneously monitored for 4 hr. On the AP side, accumulation of endogenous PGE_2 increased in a time-dependent manner. In the presence of BSP, accumulation of PGE_2 was further increased after 1 hr, and cumulative PGE_2 was significantly larger from 2 to 4 hr than that in the absence of BSP (**Fig. 6A**). BSP elevated the rate of increase of endogenous PGE_2 on the AP side from 0.041 to 0.061 pmol/hr (1.5-fold), compared to that in control cells (**Table I**). The rate of decrease of applied PGE_2-d_4 on the AP side of control cells (0.577 pmol/hr) was significantly slowed to 0.397 pmol/hr by BSP (**Table I**), and consequently the remaining amount of PGE_2-d_4 at 4 hr was increased from 49.3% to 71.3 % of the initially applied amount (**Fig. 6B**). The intracellular amount of PGE_2 in BSP-treated cells (0.220 pmol/filter) was significantly lower than that in control cells at 4 hr (0.263 pmol/filter, **Table II**). The amounts in BSP-treated and control cells accounted for 17.3 and 21.8% of the sum of PGE_2 and 15-ketoPGE_2 detected at 4 hr, respectively. On the other hand, the amounts of both PGE_2 and PGE_2-d_4 on the BL side increased in a time-dependent manner (**Figs. 6C and D**), whereas PGE_2 accumulation on the BL side was not affected by BSP (**Fig. 6C**). The average appearance rate of PGE_2-d_4 on the BL side was significantly decreased in the presence of BSP from 0.627 to 0.412 pmol/hr at 4 hr (**Table I**, **Fig. 6D**). Regardless of the presence of BSP, the increase of PGE_2-d_4 on the BL side was almost equal to its decrease on the AP side: PGE_2-d_4 decreased by 2.31 ± 0.11 and 1.59 ± 0.25 (pmol) on the AP side of untreated and BSP-treated cells, whereas it increased by 2.53 ± 0.03 and 1.61± 0.13 (pmol) in BL side, respectively. The intracellular amounts of PGE_2-d_4 in the absence and presence of BSP were 0.015 and 0.019 pmol/filter (**Table II**), which accounted for 0.33 and 0.35% of the

JPET Fast Forward. Published on November 12, 2018 as DOI: 10.1124/jpet.118.249789
This article has not been copyedited and formatted. The final version may differ from this version.

initial dose, respectively; these are not significantly different. The proportions of remaining PGE_2-d_4 in AT1-L cells were much lower than those of PGE_2, regardless of the presence of BSP (**Table II**), implying a difference in intracellular compartmentalization of endogenous and exogenous PGE_2. 15-Keto PGE_2 was detected at similar levels in both control and BSP-treated cells; however, the deuterium-labeled metabolite was not detected in the cells or the extracellular medium (**Table I, II**).

Discussion

Our present findings demonstrate that PGE_2 is transported across monolayers of primary-cultured rat AT1-L cells grown on permeable filters by OATP2A1, suggesting a contribution of OATP2A1 to PGE_2 transport from the AP to BL side of alveolar epithelium. This indicates that PGE_2 secreted to the AEL fluid in alveolar lumen (corresponding to the AP side of AT1 cells) could be re-utilized in the interstitial tissues (BL side) after vectorial transport mediated by OATP2A1 at the AP membrane in conjunction with BL MRP4. Therefore, OATP2A1 could be an important regulator of PGE_2 concentration not only in the AEL fluid, but also in the alveolar interstitial spaces.

We have previously reported cell-surface expression of Oatp2a1 in rat as well as mouse AT1-L cells (**Nakanishi et al., 2015**). We also detected robust expression of Oatp2a1 at the mRNA (**Fig. 1A**) and protein (**Fig. 1B**) levels in rat AT1-L cells used in the present study. While AT1-L cells displayed a single, distinct immunoreactive band for Oatp2a1, the rat lung tissue lysates showed additional bands of molecular sizes greater than 65 kDa. Such immunoreactive bands were also observed in the rat kidney lysates expressing a low level of Oatp2a1 and may represent more matured forms of Oatp2a1 by posttranslational modifications. The specific band observed in AT1-L cells and lung is thought to be represent de novo-synthesized Oatp2a1. Furthermore, the Km value for PGE_2 uptake by rat AT1-L cells was estimated as 43.9 nM (**Fig. 2A**), which is similar to the

JPET Fast Forward. Published on November 12, 2018 as DOI: 10.1124/jpet.118.249789
This article has not been copyedited and formatted. The final version may differ from this version.

reported K_m value of PGE_2 uptake by rat Oatp2a1 (**Kanai et al., 1995**), and the effects of Oapt2a1 inhibition were consistent with our previous findings (**Nakanishi et al., 2015**). Therefore, AT1-L cells are considered to be a reasonable experimental model to evaluate Oatp2a1 function at the alveolar epithelium. Transcellular PGE_2 transport across monolayers of rat AT1-L cells was further investigated in the present study. Apparent transcellular transport of PGE_2 was observed from the AP to the BL side, but was small in the reverse direction, indicating that PGE_2 uptake from the BL side is small (**Figs. 3A and B**). Thus, Oatp2a1 may function at the apical membranes of AT1-L cells. $P_{c,A\rightarrow B}$ of PGE_2 was significantly decreased in the presence of various OATP2A1 inhibitors, but not organic cation transporter inhibitor TEA (**Figs. 3B and D**). The K_m for AP-to-BL transport of PGE_2 (118 nM) was 2.7-fold greater than that for PGE_2 uptake by rat AT1-L cells (**Fig. 2A**), but it was close to the reported Km for rat Oatp2a1 (94 nM) (**Kanai et al., 1995**). Considering the marginal PGE_2 uptake by rat AT2 cells and Oatp2a1 expression in AT1 cells of mouse lung (**Nakanishi et al., 2015**), our current results suggest that apically expressed OATP2A1 could be the predominant contributor to trans-epithelial transport of PGE_2 in rat AT1 cells. We also observed protein expression of Mrp4 in AT1-L cells (**Fig. 1C**) and partial inhibition of PGE_2 transport by ceefourin-1 (**Fig. 4A**). The previous literature indicates that no specialized transporter is required for efflux process at the BL membranes (**Nomura et al., 2004**); however, MRP4 may contribute to cellular efflux in AT1 cells. Although we could not determine the subcellular localization of Mrp4 in rat AT1-L cells, immunoreactivity of Mrp4 has been observed in intracellular spaces of human alveolar epithelial cells (Torky et al., 2005; van der Deen et al., 2005). Further study is needed to establish in detail the mechanism of PGE_2 export in alveolar epithelium.

PGE_2 disposition in AEL fluid is mediated by different type of cells, including alveolar epithelial cells, inflammatory cells, such as alveolar macrophages, and some interstitial cells, because they can also produce PGE_2 under inflammatory conditions. The alveolar surface is mostly

JPET Fast Forward. Published on November 12, 2018 as DOI: 10.1124/jpet.118.249789
This article has not been copyedited and formatted. The final version may differ from this version.

covered with AT1 cells, so OATP2A1 may have significant role in PGE_2 disposition in the respiratory regions. Hence, in the present study, the role of Oapt2a1 in PGE_2 handling by alveolar epithelium was examined in bradykinin-treated rat AT1-L cells constitutively expressing Cox-2 and 15-Pgdh (**Fig. 5**). Externally added PGE_2-d_4 on the AP side mimics secreted or accumulated PGE_2 in the AEL fluid. Since the physiologically relevant PGE_2 concentration in AEL fluid is unknown, the PGE_2-d_4 concentration was set at 20 nM, because the dissociation constant of PGE_2 for rat EP receptors is in the range of 1 (to EP4) to 24 nM (to EP1) (**Boie et al., 1997; Dey et al., 2006**). Our transport study of PGE_2 across monolayers of rat AT1-L cells showed 1) a BSP-induced increase in AP PGE_2 concentration (**Fig. 6A and B**), 2) consistent transport of PGE_2-d_4 in the AP-to-BL direction (**Fig. 6B and D**), and 3) predominant secretion of PGE_2 toward the BL side (**Fig. 6A and C**). Given the dominant role of Oatp2a1 in PGE_2 uptake from the AP side of AT1-L cells, impaired function of OATP2A1 may result in an increase of PGE_2 concentration in the AEL fluid due to elevated PGE_2 secretion, reflecting reduced reuptake and decreased transport of pooled/secreted PGE_2 in AEL. This observation agrees well with a report of elevated PGE_2 level in BAL of bleomycin-administered *Sclo2a1*$^{-/-}$ mice (**Nakanishi et al., 2015**).

Our study also showed that PGE_2 on the AP side of cells could be transported to the BL side without being metabolized, because the increase in the remaining amount of exogenous PGE_2 in the presence of BSP was counterbalanced by the decrease in its amount on the BL side. Indeed, much less PGE_2-d_4 (approximately 0.3%) than PGE_2 (17.5 - 21.7%) remained in cells, and no metabolite of PGE_2-d_4 was found in either cells or extracellular medium (**Table I**), although 15-Pgdh expression was observed in AT1-L cells (**Fig. 5**) and 15-ketoPGE_2 was collected from the cells (**Table II**). This observation clearly suggests that the distribution of exogenous PGE_2 is distinct from that of newly synthesized PGE_2, and this can be explained by much faster transfer of exogenous PGE_2 across the cell monolayer as compared to the rate of metabolism by intracellular

15-Pgdh. Thus, trans-epithelial transport of secreted PGE_2 in alveolar lumen can be regarded as "re-secretion" toward the BL side of the cells, to which Oatp2a1 and Mrp4 both contribute. This idea is illustrated in **Fig. 7**, although the subcellular localization of Mrp4 still needs to be verified. This could provide a route for rapid transfer of PGE_2 into interstitial tissues in the lung. This would be consistent with the reported transport of PGE_2 in MDCK cells transfected with h*SLCO2A1* (**Nomura et al., 2004**) and murine collecting duct cells in the kidney (**Chi et al., 2008**). Our present study is the first demonstration of this concept in primary-cultured cells. Thirdly, it is noteworthy that the cumulative amount of PGE_2 at 4 hr on the BL side (0.62 ± 0.02 pmol) was approximately 2.6 times higher than that on the AP side (0.24 ± 0.02 pmol) in control cells (**Fig. 6C**), implying polarized secretion of PGE_2. To date, little is known about such asymmetrical secretion of PGE_2 from cells. Our results showed that BSP increased the AP accumulation of PGE_2 (produced by AT1-L cells) by 0.07 pmol (**Fig. 6A**); however, the difference did not simply reflect the reduction of PGE_2 accumulation on the BL side (**Fig. 6C**), in contrast to the case of PGE_2-d_4 (**Fig. 6B and D**). Further study is needed to establish how intracellularly synthesized PGE_2 is handled by cells.

We previously showed that intratracheally bleomycin-administered *Slco2a1*$^{-/-}$ mice exhibit more severe pulmonary fibrosis than wild-type counterparts. Aggravated fibrosis in *Slco2a1*$^{-/-}$ mice was associated with an elevated level of PGE_2 in bronchoalveolar lavage fluid and increased phosphorylation of profibrotic protein kinase C (PKC)-δ in the lung tissue (**Nakanishi et al., 2015**). Previous research has suggested that extracellular PGE_2 suppresses PKC-δ activation, which contributes to collagen production in lung fibroblasts (**Huang et al., 2008**). Based on our present findings, OATP2A1-mediated PGE_2 transport to the interstitial space from AEL fluid may contribute to modulation of PKC-δ activity in fibroblasts. Taken together, these results may provide a new rationale for the enhanced PKC-δ activity in aggravated fibrosis of *Slco2a1*$^{-/-}$ mice.

In conclusion, our study demonstrates that apically expressed OATP2A1 contributes to transcellular transport of PGE_2 across monolayers of rat AT1-L cells. OATP2A1 apparently reduces secretion of endogenous PGE_2 on the AP side and facilitates "re-secretion" of exogenous PGE_2 on the BL side of AT1-L cells. This may be an important mechanism for transferring existing PGE_2 from AEL fluid to intestinal space or blood, thereby contributing to not only efficient elimination of PGE_2 from alveolar lumen, but also to the modulation of PGE_2 signaling of interstitial cells, such as fibroblasts. A detailed understanding of this role of OATP2A1 in the progression of interstitial pneumonia may provide with a clue to develop new therapeutic strategies for pulmonary fibrosis.

Acknowledgment

We thank Ms. Sakiyama and Dr. Gose for their technical assistance.

Authorship Contributions

Participated in research design: Nakanishi, Takashima and Tamai.

Conducted experiments: Nakanishi, Takashima, Uetoko, and Komori.

Contributed new reagents or analytic tools: Nakanishi, Takashima, and Uetoko.

Performed data analysis: Nakanishi, Takashima, Uetoko and Komori.

Wrote or contributed to the writing of the manuscript: Nakanishi, Komori and Tamai.

References

Boie Y, Stocco R, Sawyer N, Slipetz DM, Ungrin MD, Neuschafer-Rube F, Puschel GP, Metters KM and Abramovitz M (1997) Molecular cloning and characterization of the four rat prostaglandin E2 prostanoid receptor subtypes. *Eur J Pharmacol* **340**:227-241.

Bonner JC, Rice AB, Ingram JL, Moomaw CR, Nyska A, Bradbury A, Sessoms AR, Chulada PC, Morgan DL, Zeldin DC and Langenbach R (2002) Susceptibility of cyclooxygenase-2-deficient mice to pulmonary fibrogenesis. *Am J Pathol* **161**:459-470.

Chan BS, Satriano JA, Pucci M and Schuster VL (1998) Mechanism of prostaglandin E2 transport across the plasma membrane of HeLa cells and Xenopus oocytes expressing the prostaglandin transporter "PGT". *J Biol Chem* **273**:6689-6697.

Chang HY, Locker J, Lu R and Schuster VL (2010) Failure of postnatal ductus arteriosus closure in prostaglandin transporter-deficient mice. *Circulation* **121**:529-536.

Chen C and Klaassen CD (2004) Rat multidrug resistance protein 4 (Mrp4, Abcc4): molecular cloning, organ distribution, postnatal renal expression, and chemical inducibility. *Biochem Biophys Res Commun* **317**:46-53.

Cheung L, Flemming CL, Watt F, Masada N, Yu DM, Huynh T, Conseil G, Tivnan A, Polinsky A, Gudkov AV, Munoz MA, Vishvanath A, Cooper DM, Henderson MJ, Cole SP, Fletcher JI, Haber M and Norris MD (2014) High-throughput screening identifies Ceefourin 1 and Ceefourin 2 as highly selective inhibitors of multidrug resistance protein 4 (MRP4). *Biochem Pharmacol* **91**:97-108.

Chi Y, Khersonsky SM, Chang YT and Schuster VL (2006) Identification of a new class of prostaglandin transporter inhibitors and characterization of their biological effects on prostaglandin E2 transport. *J Pharmacol Exp Ther* **316**:1346-1350.

Chi Y, Pucci ML and Schuster VL (2008) Dietary salt induces transcription of the prostaglandin transporter gene in renal collecting ducts. *Am J Physiol Renal Physiol* **295**:F765-F771.

Dey I, Lejeune M and Chadee K (2006) Prostaglandin E2 receptor distribution and function in the gastrointestinal tract. *Br J Pharmacol* **149**:611-623.

Ferreira SH and Vane JR (1967) Prostaglandins: Their Disappearance from and Release into the Circulation. *Nature* **216**:868-873.

Gose T, Nakanishi T, Kamo S, Shimada H, Otake K and Tamai I (2016) Prostaglandin transporter (OATP2A1/SLCO2A1) contributes to local disposition of eicosapentaenoic acid-derived PGE. *Prostaglandins Other Lipid Mediat* **122**:10-17.

Huang S, Wettlaufer SH, Hogaboam C, Aronoff DM and Peters-Golden M (2007) Prostaglandin E(2) inhibits collagen expression and proliferation in patient-derived normal lung fibroblasts via E prostanoid 2 receptor and cAMP signaling. *Am J Physiol Lung Cell Mol Physiol* **292**:L405-L413.

Huang SK, Wettlaufer SH, Chung J and Peters-Golden M (2008) Prostaglandin E2 inhibits specific lung fibroblast functions via selective actions of PKA and Epac-1. *Am J Respir Cell Mol Biol* **39**:482-489.

Ikehata M, Yumoto R, Nakamura K, Nagai J and Takano M (2008) Comparison of albumin uptake in rat alveolar type II and type I-like epithelial cells in primary culture. *Pharm Res* **25**:913-922.

Kamo S, Nakanishi T, Aotani R, Nakamura Y, Gose T and Tamai I (2017) Impact of FDA-Approved Drugs on the Prostaglandin Transporter OATP2A1/SLCO2A1. *J Pharm Sci* **106**:2483-2490.

Kanai N, Lu R, Satriano JA, Bao Y, Wolkoff AW and Schuster VL (1995) Identification and characterization of a prostaglandin transporter. *Science* **268**:866-869.

Keerthisingam CB, Jenkins RG, Harrison NK, Hernandez-Rodriguez NA, Booth H, Laurent GJ, Hart SL, Foster ML and McAnulty RJ (2001) Cyclooxygenase-2 deficiency results in a loss of the anti-proliferative response to transforming growth factor-beta in human fibrotic lung fibroblasts and promotes bleomycin-induced pulmonary fibrosis in mice. *Am J Pathol* **158**:1411-1422.

Kimura H, Takeda M, Narikawa S, Enomoto A, Ichida K and Endou H (2002) Human organic anion transporters and human organic cation transporters mediate renal transport of prostaglandins. *J Pharmacol Exp Ther* **301**:293-298.

Kolodsick JE, Peters-Golden M, Larios J, Toews GB, Thannickal VJ and Moore BB (2003) Prostaglandin E2 inhibits fibroblast to myofibroblast transition via E. prostanoid receptor 2 signaling and cyclic adenosine monophosphate elevation. *Am J Respir Cell Mol Biol* **29**:537-544.

Lovgren AK, Jania LA, Hartney JM, Parsons KK, Audoly LP, Fitzgerald GA, Tilley SL and Koller BH (2006) COX-2-derived prostacyclin protects against bleomycin-induced pulmonary fibrosis. *Am J Physiol Lung Cell Mol Physiol* **291**:L144-L156.

Lu R, Kanai N, Bao Y and Schuster VL (1996) Cloning, in vitro expression, and tissue distribution of a human prostaglandin transporter cDNA(hPGT). *J Clin Invest* **98**:1142-1149.

Maher TM, Evans IC, Bottoms SE, Mercer PF, Thorley AJ, Nicholson AG, Laurent GJ, Tetley TD, Chambers RC and McAnulty RJ (2010) Diminished prostaglandin E2 contributes to the apoptosis paradox in idiopathic pulmonary fibrosis. *Am J Respir Crit Care Med* **182**:73-82.

Moore BB, Ballinger MN, White ES, Green ME, Herrygers AB, Wilke CA, Toews GB and Peters-Golden M (2005) Bleomycin-induced E prostanoid receptor changes alter fibroblast responses to prostaglandin E2. *J Immunol* **174**:5644-5649.

Nakanishi T, Hasegawa Y, Mimura R, Wakayama T, Uetoko Y, Komori H, Akanuma S, Hosoya K and Tamai I (2015) Prostaglandin Transporter (PGT/SLCO2A1) Protects the Lung from Bleomycin-Induced Fibrosis. *PLoS One* **10**:e0123895.

Nakanishi T, Ohno Y, Aotani R, Maruyama S, Shimada H, Kamo S, Oshima H, Oshima M, Schuetz JD and Tamai I (2017) A novel role for OATP2A1/SLCO2A1 in a murine model of colon cancer. *Sci Rep* **7**:16567.

Nomura T, Lu R, Pucci ML and Schuster VL (2004) The two-step model of prostaglandin signal termination: In vitro reconstitution with the prostaglandin transporter and prostaglandin 15 dehydrogenase. *Mol Pharmacol* **65**:973-978.

Oga T, Matsuoka T, Yao C, Nonomura K, Kitaoka S, Sakata D, Kita Y, Tanizawa K, Taguchi Y, Chin K, Mishima M, Shimizu T and Narumiya S (2009) Prostaglandin F(2alpha) receptor signaling facilitates bleomycin-induced pulmonary fibrosis independently of transforming growth factor-beta. *Nat Med* **15**:1426-1430.

Pucci ML, Bao Y, Chan B, Itoh S, Lu R, Copeland NG, Gilbert DJ, Jenkins NA and Schuster VL (1999) Cloning of mouse prostaglandin transporter PGT cDNA: species-specific substrate affinities. *Am J Physiol Renal Physiol* **277**:R734-R741.

Reid G, Wielinga P, Zelcer N, van der Heijden I, Kuil A, de Haas M, Wijnholds J and Borst P (2003) The human multidrug resistance protein MRP4 functions as a prostaglandin efflux transporter and is inhibited by nonsteroidal antiinflammatory drugs. *Proc Natl Acad Sci USA* **100**:9244-9249.

Richards RJ, Davies N, Atkins J and Oreffo VI (1987) Isolation, biochemical characterization, and culture of lung type II cells of the rat. *Lung* **165**:3.

Schuster VL (1998) Molecular mechanisms of prostaglandin transport. *Annu Rev Physiol* **60**:221-242.

Sekine T, Watanabe N, Hosoyamada M, Kanai Y and Endou H (1997) Expression cloning and characterization of a novel multispecific organic anion transporter. *J Biol Chem* **272**:18526-18529.

Shimada H, Nakamura Y, Nakanishi T and Tamai I (2015) OATP2A1/SLCO2A1-mediated prostaglandin E loading into intracellular acidic compartments of macrophages contributes to exocytotic secretion. *Biochem Pharmacol* **98**:629-638.

Syeda MM, Jing X, Mirza RH, Yu H, Sellers RS and Chi Y (2012) Prostaglandin transporter modulates wound healing in diabetes by regulating prostaglandin-induced angiogenesis. *Am J Pathol* **181**:334-346.

Tamai I, Nezu J-i, Uchino H, Sai Y, Oku A, Shimane M and Tsuji A (2000) Molecular identification and characterization of novel members of the human organic anion transporter (OATP) family. *Biochem Biophys Res Commun* **273**:251-260.

Torky AR, Stehfest E, Viehweger K, Taege C and Foth H (2005) Immuno-histochemical detection of MRPs in human lung cells in culture. *Toxicology* **207**:437-450.

van der Deen M, de Vries EG, Timens W, Scheper RJ, Timmer-Bosscha H and Postma DS (2005) ATP-binding cassette (ABC) transporters in normal and pathological lung. *Respir Res* **6**:59.

Footnotes

This work was supported by the Grant-in-Aid for Scientific Research [KAKENHI 15H04755 to TN]; and the Japan Society for the Promotion of Science and the Smoking Research Foundation [Grant 055 to TN].

JPET Fast Forward. Published on November 12, 2018 as DOI: 10.1124/jpet.118.249789
This article has not been copyedited and formatted. The final version may differ from this version.

Figure Legends

Figure 1 Expression of transporter genes in rat AT1-L cells

(A) PCR was repeated at three times with three independently cultured lots of AT1-L cells. Bands were visualized with ethidium bromide after electrophoresis on 1.5 % agarose gel. Primers used are listed in Supplementary Table I. (B) and (C) Western blotting was performed for Oatp2a1 (B) and Mrp4 (C) in rat AT1-L cells. Rat lung and kidney homogenates were utilized as positive controls for Oatp2a1 and Mrp4, respectively. Experiments were repeated three times with two separately prepared lots of AT1-L cells, and representative Western blots are shown.

Figure 2 PGE_2 uptake by AT1-L cells

(A) Saturation kinetics of PGE_2 uptake by AT1-L cells was analyzed according to the Michaelis-Menten equation. Experiments were repeated multiple times and each point represents the mean value ± S.E.M. of three separate cell lots. The inset shows an Eadie-Hofstee plot of the data. (B) PGE_2 uptake by AT1-L was evaluated in the absence (Cont) or presence of BSP, TGBz or unlabeled PGE_2 at 25 μM. Each bar represents the mean value of three individual cell lots with S.E.M. Statistical analysis was conducted by one-way ANOVA with Bonferroni's multiple comparisons test: *** indicates $p < 0.001$. NS: no significant difference.

Figure 3 Characterization of PGE_2 transport across monolayers of AT1-L cells

(A) Transport of [^{3}H]PGE_2 (2.78 nM) was monitored in the short term. Open and closed symbols indicate cumulative amounts of [^{3}H]PGE_2 in the absence and the presence of 25 μM BSP. Experiments were repeated at least three times, and each point represents the mean of three results from separate cell lots with S.E.M. (B) Effect of BSP on P_c of PGE_2 and mannitol. P_c was evaluated

JPET Fast Forward. Published on November 12, 2018 as DOI: 10.1124/jpet.118.249789
This article has not been copyedited and formatted. The final version may differ from this version.

for transcellular transport of [^{3}H]PGE_2 and [^{14}C]mannitol in the absence (Cont) or in the presence of BSP (25 μM). Each bar represents the mean of three results from separate cell lots with S.E.M. (C) Saturation kinetics of AP-to-BL transport of PGE_2. Experiments were repeated three times and all data was plotted, and analyzed according to the Michaelis-Menten equation. (D) Effects of various compounds on $P_{c,A\rightarrow B}$ of PGE_2. The values were obtained in the absence (Cont) or in the presence of TGBz and or suramin (25 μM), or TEA (100 μM). Each bar represents the mean of three results from separate cell lots with S.E.M. One-way ANOVA with Bonferroni's multiple comparisons test was used: *** indicates $p < 0.001$. NS: no significant difference.

Figure 4 Characterization of PGE_2 transport across monolayers of AT1-L cells

(A) Effect of ceefourin-1 on P_c of PGE_2. P_c was evaluated in transcellular transport of [^{3}H]PGE_2 in the absence (Cont) or the presence of ceefourin-1 at the indicated concentration. Each bar represents the mean of three results from individual cell lots with S.E.M. Statistical analysis was conducted with Student's t-test: ** indicates $P < 0.01$. (B) Effect of ceefourin-1 on PGE_2 uptake by HEK/2A1 cells overexpressing human OATP2A1. Statistical analysis was conducted by one-way ANOVA with Bonferroni's multiple comparisons test. ** indicates $p < 0.05$. NS: no significant difference.

Figure 5 Western blot for Cox-2 and 15-Pgdh in rat AT1-L cells.

Western blotting was performed for Cox-2 and Pgdh in rat lung and primary cultured alveolar epithelial cells. Experiments were repeated three times with separately prepared lots of AT1-L cells. Representative Western blots are shown.

Figure 6 Effect of BSP on PGE_2 and PGE_2-d_4 disposition.

Effect of BSP on accumulation of endogenous PGE_2 (A) and remaining PGE_2-d_4 (B) on the AP side and on accumulation of PGE_2 (C) and PGE_2-d_4 (D) in cells with (closed circles) and without (open circles) BSP. Each point represents the mean of results from six separate cell lots with S.E.M. Statistical analysis was conducted with Student's t-test: ** indicates $P < 0.01$.

Figure 7 Hypothesized roles of Oatp2a1 and Mrp4 in transcellular PGE2 transport.

PGE_2 secreted into alveolar lumen by alveolar epithelial cells, inflammatory cells and alveolar macrophages can be taken up by OATP2A1 expressed at apical membranes of AT1 cells, and transferred into interstitial space in cooperation with MRP4, where PGE_2 exerts it anti-fibrotic action against fibroblasts.

Table I Rates of change of PGE_2 and PGE_2-d_4 in the presence and absence of BSP

	AP side [a)] (pmol/hr/filter)		BL side (pmol/hr/filter)	
	Control	+BSP	Control	+BSP
PGE_2	0.041 ± 0.003	0.061 ± 0.004 **	0.148 ± 0.005	0.161 ± 0.014
PGE_2-d_4	-0.577 ±0.032	-0.397 ± 0.052 *	0.627 ± 0.011	0.412 ± 0.032 ***

Samples were collected from extracellular medium containing 10 μM bradykinin. Metabolites of PGE_2 and PGE_2-d_4 were not detected in extracellular medium.

a) A minus sign indicate rate of decrease of PGE_2 or PGE_2-d_4.

Results show the mean value ± S.E.M. of six wells.

Statistical analysis was conducted with Student's t-test compared to Control: *, **, and *** indicates $P < 0.05$, 0.01 and 0.001, respectively.

Table II

Intracellular accumulation of PGE_2 and its metabolite 15-ketoPGE$_2$

	Control				+BSP			
	Intact (pmol)	% [a]	Metabolite [b] (pmol)	% [a]	Intact (pmol)	% [a]	Metabolite [b] (pmol)	% [a]
PGE_2	0.263 ± 0.009	21.7 ± 0.77	0.088 ± 0.004	7.3 ± 0.47	0.220 ± 0.007 **	17.3 ± 0.58 **	0.107 ± 0.006 *	8.50 ± 0.59
PGE_2-d_4	0.015 ± 0.005	0.33 ± 0.10	N.D.	N.D.	0.019 ± 0.002	0.35 ± 0.20	N.D.	N.D.

a) Proportions of PGE_2 and PGE_2-d_4, were calculated based on the sum of PGE_2 and 15-ketoPGE$_2$ at 4 hr (1.21 pmol for control cells, and 1.26 pmol for BSP-treated AT1-L cells), and the initial dose of PGE_2-d_4 (4.55 pmol for control cells, and 5.54 for BSP-treated cells), as determined by LC/MS-MS.

b) The only metabolite detected was 15-ketoPGE$_2$.

N.D.; not detected.

Results show the mean value ± S.E.M. of six wells.

Statistical analysis was conducted with Student's t-test compared to Control: * and ** indicate $P < 0.05$ and 0.01, respectively.

Figure 1

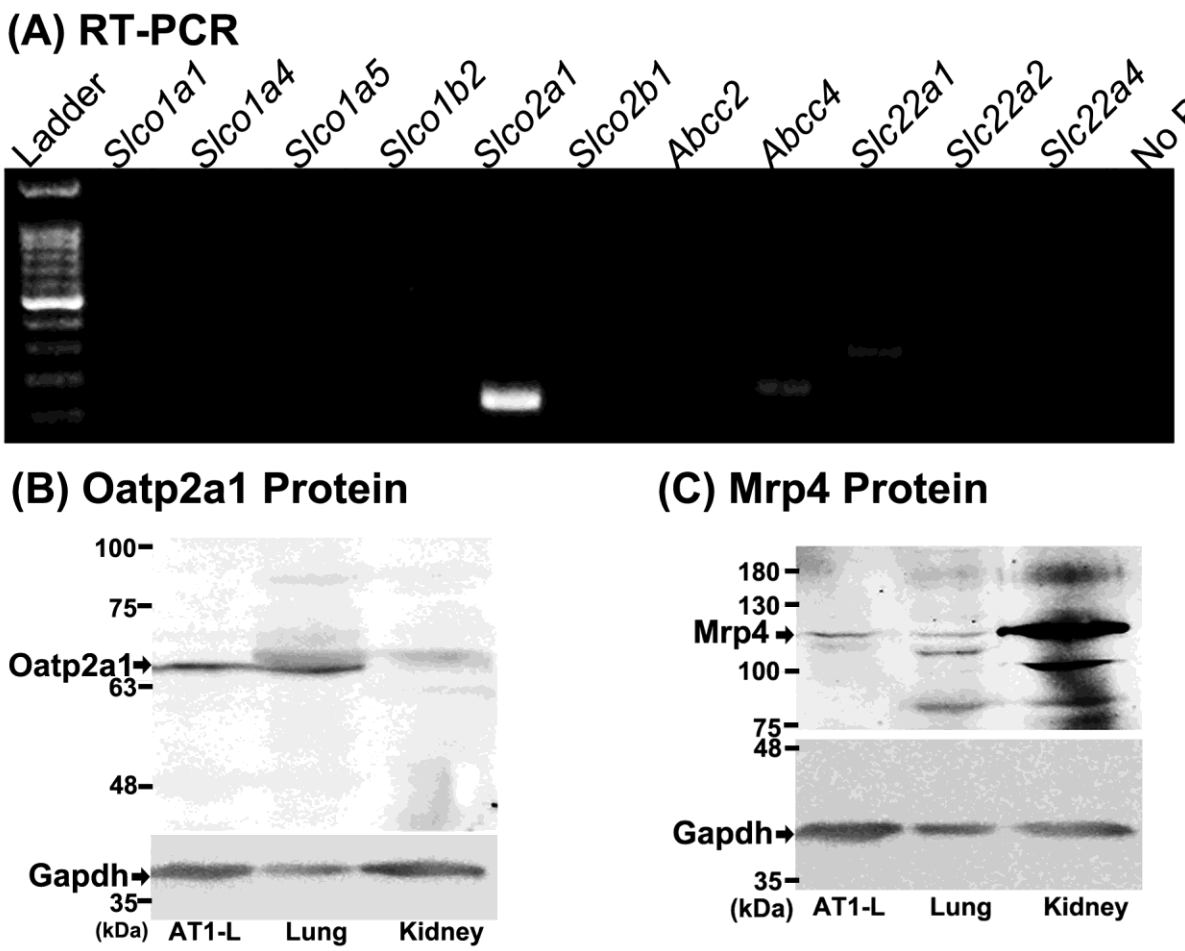

Figure 2

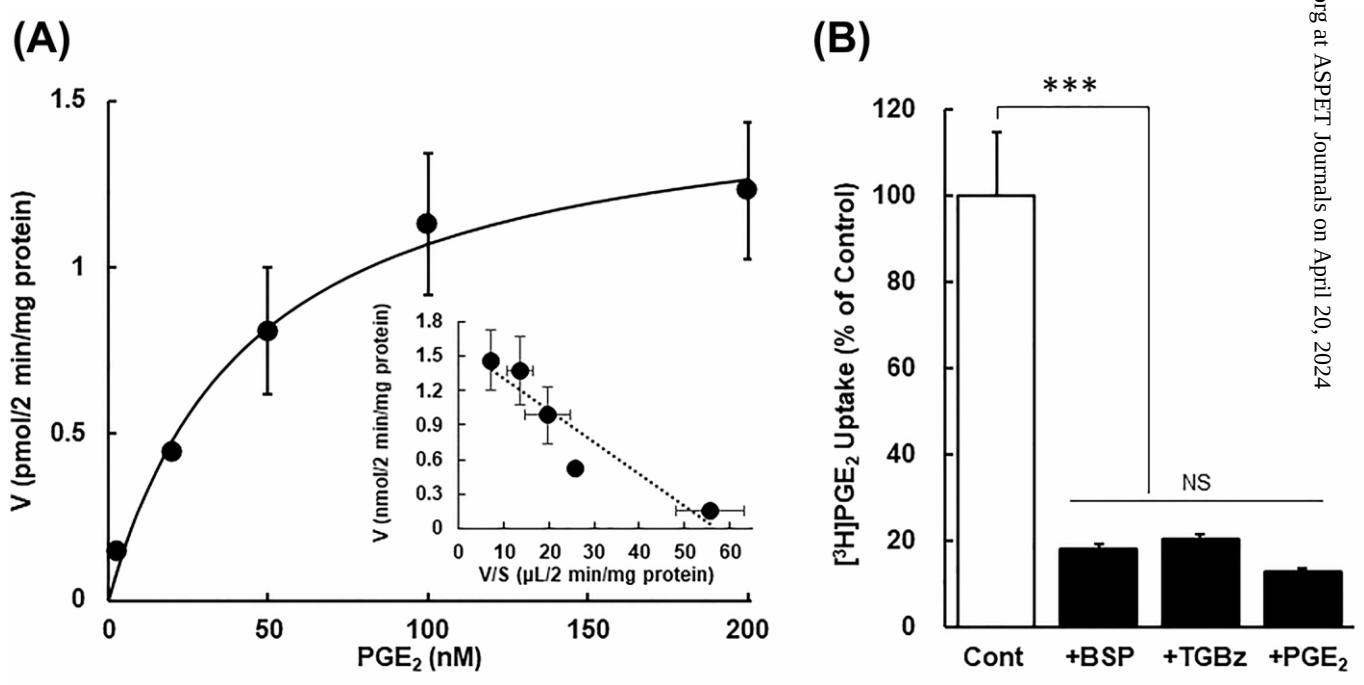

Figure 3

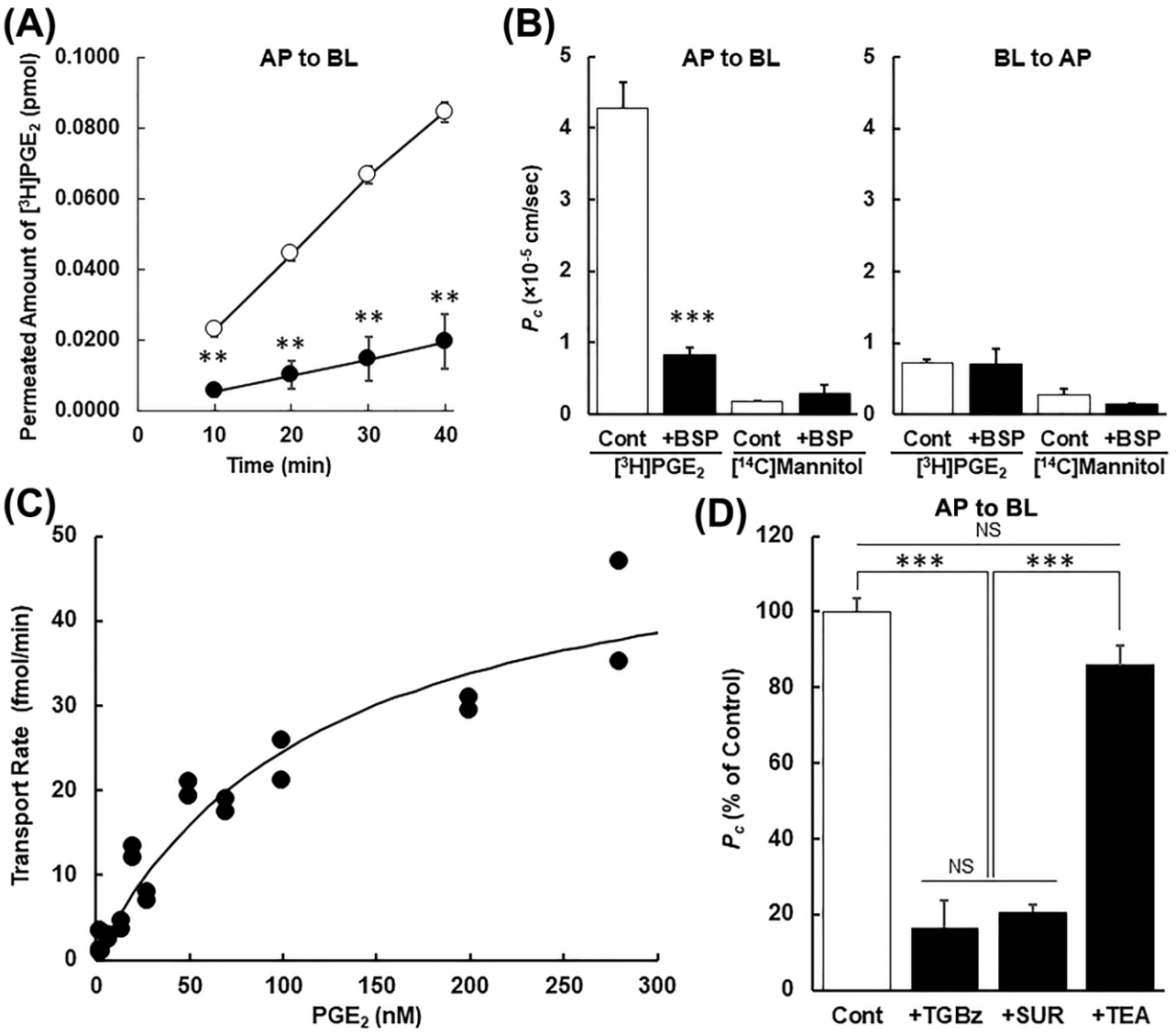

Figure 4

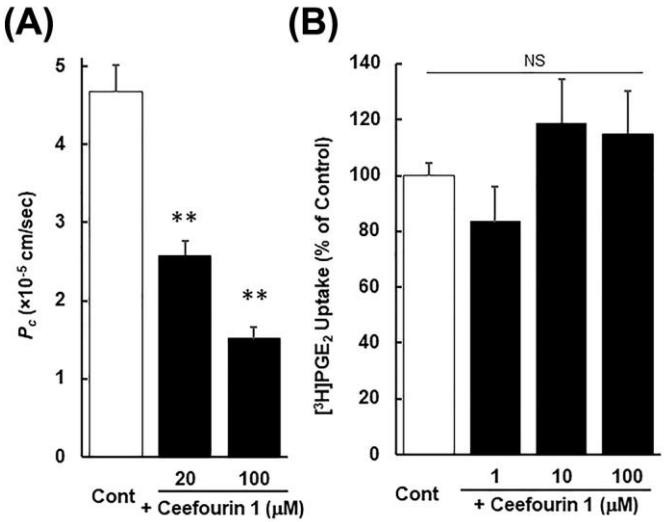

Figure 5

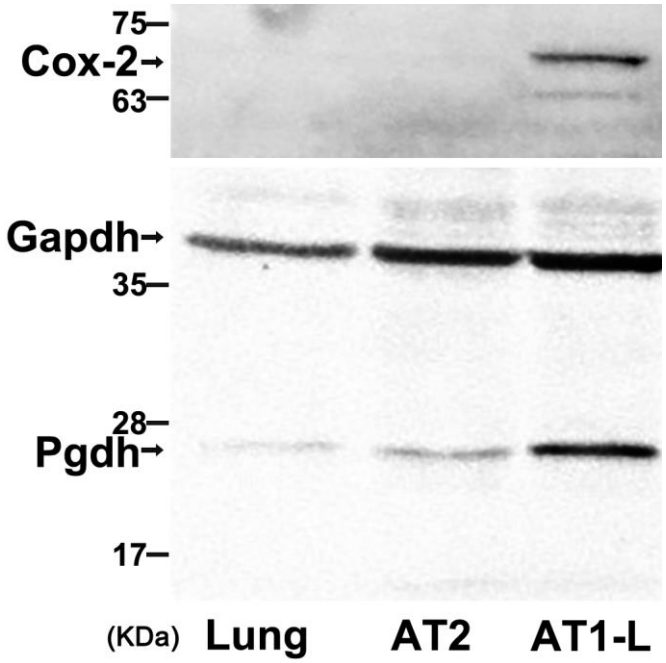

Figure 6

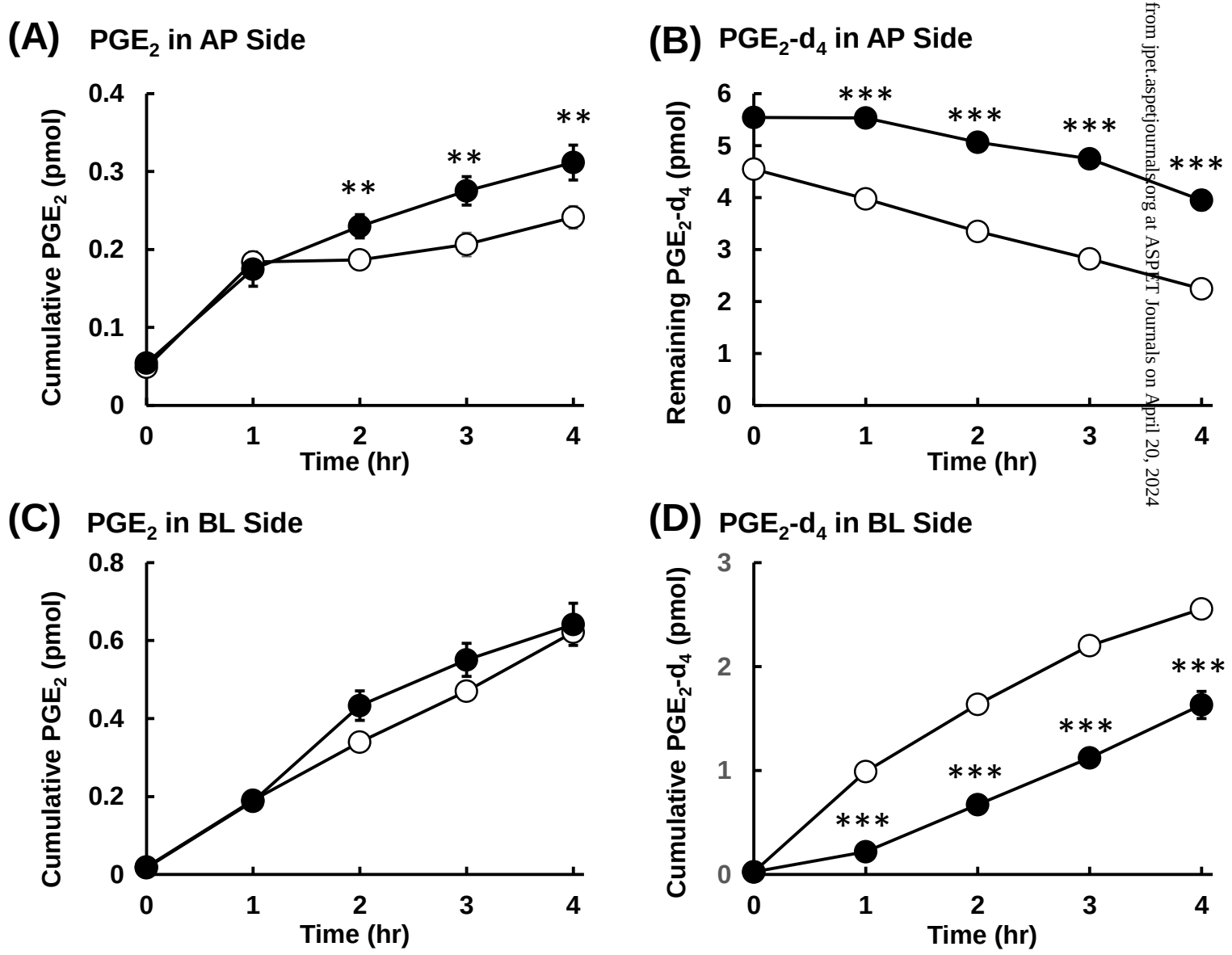

Figure 7